# Strain-engineered interaction of quantum polar and superconducting phases

Chloe Herrera,[1] Jonah Cerbin,[1] Amani Jayakody,[1] Kirsty Dunnett,[2] Alexander V. Balatsky,[1,2] and Ilya Sochnikov[1,3,*]

[1]*Physics Department, University of Connecticut, 196 Auditorium Road, Storrs, Connecticut 06269, USA*

[2]*Nordita, KTH Royal Institute of Technology and Stockholm University, Roslagstullsbacken 23, SE-106 91 Stockholm, Sweden*

[3]*Institute of Material Science, University of Connecticut, 97 North Eagleville Road, Storrs, Connecticut 06269, USA*

(Received 10 June 2019; revised manuscript received 23 November 2019; published 26 December 2019)

The pairing mechanism of unconventional superconductivity in strontium titanate is hotly debated. Here, using a multisensor experimental apparatus with a mechanical strain cell, an optical microscope, and with transport and magnetic probes all contained in a closed-cycle dilution refrigerator, we determined that the superconducting transition temperature of strontium titanate increases dramatically even for very small strains induced by application of uniaxial tension. These results imply that superconductivity is controlled by very small atomic shifts; the only strain-sensitive pairing channel candidate is the one linked to quantum ferroelectric (polar) instability. This investigation, therefore, uncovers additional constraints on the debated theories of superconductivity in this low carrier concentration material near the ferroelectric quantum phase transition.

DOI: 10.1103/PhysRevMaterials.3.124801

## I. INTRODUCTION

The major open question of the mechanism of superconducting pairing in strontium titanate (STO) has stimulated vigorous debate [1–12]. Recent experimental works have demonstrated the enhancement of superconductivity in STO via changes in crystal composition or epitaxy [13–16], and they have revealed the potential importance of the ferroelectric (FE) quantum phase transition to this material's unusual phonon behavior [17–21] and mysterious electron pairing [3,7,22–28,13,14,10,29–33]. One of the debated aspects is which phonons provide the pairing glue: longitudinal optical phonons with energies that can be larger than the Fermi energy, or the FE transverse optical modes with energy that can be lower than the Fermi energy. From here the debate splits into treating STO as either the antiadiabatic limit or as a standard BCS limit but considering only some low-energy phonons. From here the debate continues to a consideration of the exact microscopic origin of the strong electron-phonon coupling in the above phonon branches: single phonon, polaronic, the more recent two-phonon [12], and all-phonon-inclusive proposals [34]. An additional complication is the antiferrodistortive (AFD) order, which generally has not been considered as influencing superconductivity in many experiments and in *all* existing theories.

In summary, no single theory has conclusively explained the microscopic pairing mechanism of superconductivity in STO. We believe that experiments that precisely control both the FE and AFD orders are necessary to guide future theoretical efforts. To address this fundamental challenge, here we performed an experiment in which lattice properties were changed in a controlled way, enabling us to accurately probe the origin of superconductivity in STO and its relation to structural changes and instabilities. We applied a previously unexplored tensile $(001)_t$ stress approach and observed a large enhancement of the critical temperature ($T_c$) in STO, which we interpret as originating in softening (Fig. 1 of this paper and Fig. S1 of the Supplemental Material [76]) of the transverse FE mode [35–39]. Softening of the mode under tension could prompt strong changes in electronic behavior even at small subpicometer deformations [40]. Note that our experiment indicates that the strong interplay between the AFD and FE modes is an important parameter. Within the tensile deformation geometry investigated here, the AFD and FE modes are expected to work in synchrony [41] and thus may strongly increase $T_c$, as anticipated in FE soft-mode scenarios [3,7]. The longitudinal optical FE phonon mode does not respond directly to stress [35]; therefore, models involving longitudinal optical modes are difficult to reconcile with our experimental findings, unless some completely new, unexplored theoretically secondary process is involved.

## II. EXPERIMENTAL APPROACH

To elucidate the role of lattice modes in superconductivity in STO, we applied uniaxial compressive and tensile stresses—a clean nonchemical control [33,42–44]—to narrow thin bars of $SrTi_{1-x}Nb_xO_3$ crystals (Nb-doped STO), and we measured the resistive and magnetic signatures of the superconducting transition. Our experimental setup [Fig. 1(a) and Figs. S2–S6] consisted of a home-built strain cell and a polarizing optical microscope installed in a dilution refrigerator, as detailed elsewhere [45]. While we applied (unmeasured) uniaxail stress, we measured the resultant strain along the stress direction using gauges attached to the samples [Fig. 1(b)]. The strain, $\varepsilon_{zz}$, along the long side of the thin and narrow crystals [Fig. 1(b)] reported in the following figures was typically measured at ∼50 mK. This work reports data from six independent samples that exhibited an increase in the superconducting transition temperature, $T_c$, upon tensile $[001]_t$ stress. We used very low excitation currents (100 nA

*ilya.sochnikov@uconn.edu

 

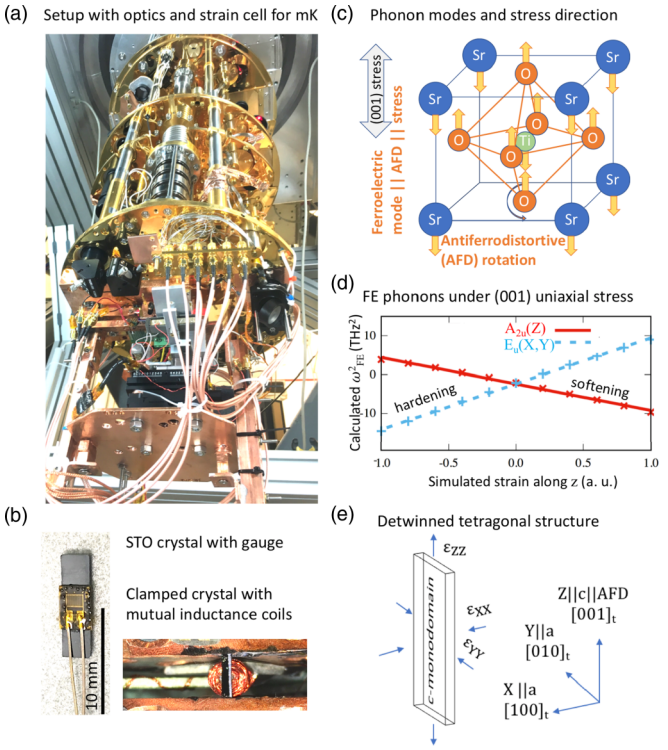


FIG. 1. Experimental setup and expected FE phonon mode softening in STO under the stress-strain conditions used here. (a) Apparatus based on a closed-cycle dilution refrigerator with a base temperature of 7 mK. Electronic transport, mutual inductance, and optical measurements were performed *in situ* while the strain was continuously tuned [45]. (b) Long, narrow, and thin samples (left image; typically $10 \times 2 \times 0.27\,\mathrm{mm}^3$) were clamped (right image) in the custom strain cell to apply tunable strain monitored along the long side of the crystals using the shown flexible strain gauge. (c) Schematic of atomic vibrations of the FE phonon mode and its alignment with the AFD $c$-axis for stress along $[001]_t$. (d) Calculated softening of the $A_{2u}(Z)$ FE phonon mode parallel to the AFD rotation axis and hardening of the $E_u(X,Y)$ mode perpendicular to the AFD axis, under uniaxial $[001]_t$ tensile stress (based on Ref. [7]). (e) Strain in the $Z$ direction, $\varepsilon_{ZZ}$, measured by the gauge has the opposite sign to the coinduced $X$ and $Y$ strains, $\varepsilon_{XX}$ and $\varepsilon_{YY}$, which can be determined using Poisson's ratio [47]. The sample geometry promotes $c$-domains, which are fully detwinned by the [001] tensile stress; a larger stress corresponding to the induced strain along the $[001]_t$ direction of the detwinned crystal is expected to soften the FE phonon mode.

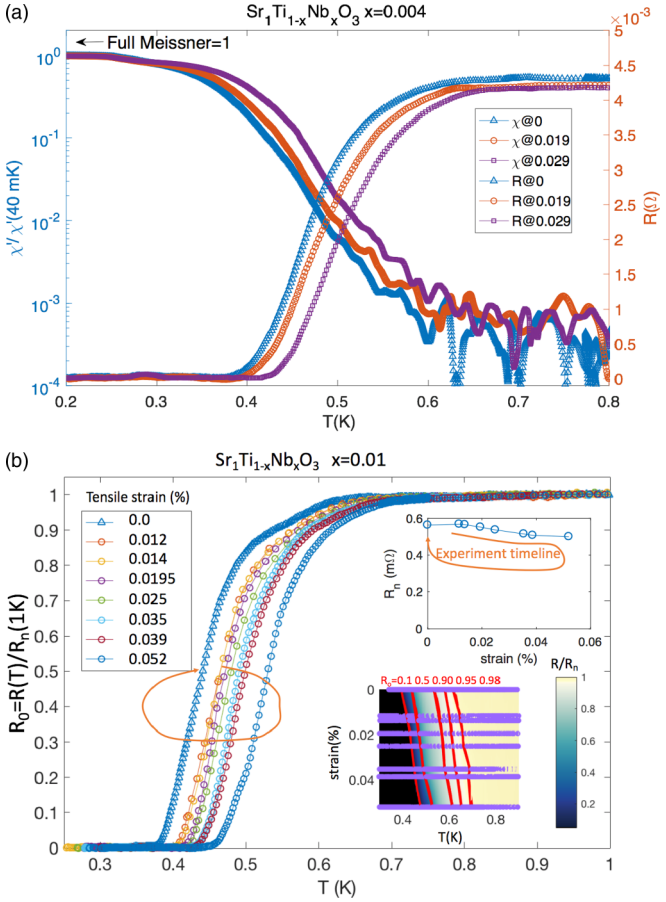


FIG. 2. Large enhancement of $T_c$ under uniaxial $(001)_t$ tensile stress in $SrTi_{1-x}Nb_xO_3$ as confirmed by magnetic susceptibility and resistive probes. (a) Magnetic susceptibility, reflecting the screening fraction, and resistive transitions shift toward higher temperature upon tensile stress; these two parameters were measured simultaneously for a sample with $x = 0.004$. Three measured $\varepsilon_{ZZ}$ values of strain are indicated in %. The susceptibility data are the three down-turning curves, from full Meissner to no screening (left ordinate). The resistance data are the three up-turning curves, from zero to normal resistance of a few mΩ. The screening signal extends all the way into the resistive drop. Both the diamagnetic screening and the resistive shifts in the transition happen in the same manner, which rules out trivial filamentary superconductivity under stress and indicates a large strain effect on the bulk transition temperature regardless of the specific definition of the transition temperature. (b) Resistive transition for the sample with $x = 0.01$. Curves are normalized to the resistance at 1 K, $R_n$. The upper inset "Experimental timeline" traces $R_n$: the sample measurements start from nonzero as-cooled strain of 0.011% (the beginning of the arrow); next, the normal resistance reduces slightly at increasing tensile strain values; finally, the resistance value returns to the original value after the release of strain (at the arrowhead, 0%). The reversibility demonstrates that the critical temperature change is not driven by the formation of permanent lattice defects. The lower inset shows the enhancement of $T_c$ and the almost constant width of the transition under different strains; the enhancement is independent of the definitions of $T_c$ (emphasized on the colormap by the red $R_0 =$ const lines).

to 100 $\mu$A) and an ultralow noise amplifier and a resistance bridge to measure the resistive phase transition, with a signal level of hundreds of picovolts. Mutual inductance coils were installed in the strain cell to measure the magnetic signatures of the transition ([46] and the Supplemental Material [76]).

In this paper, we use square brackets to denote a crystallographic axis and round brackets to denote a crystallographic plane, e.g., [001] and (001), respectively. The $a = b$ tetragonal lattice sides are along the $[100]_t$ and $[010]_t$ directions. The longer $c$ lattice side ($c$-axis) is in the $[001]_t$ direction [Figs. 1(c)–1(e)]. The subscript $t$ is used to emphasize the tetragonal (monodomain) phase. No subscript denotes directions in the high-temperature cubic phase. This convention is similar to that used previously in Ref. [35].

## III. RESULTS

Typical resistive transitions for various Nb contents are given in Figs. 2 and 3(a)–3(d). We observed significant and reversible increases in the critical temperature of $SrTi_{1-x}Nb_xO_3$ under tensile strain [Figs. 2(a) and 2(b)]. When sufficiently large strains were achieved, we observed a dramatic nonlinear upturn toward higher temperatures [Figs. 3(b) and 3(c)]. The entire resistive transitions were considered, and the temperatures at which the resistance was 10%, 50%, 90%, 95%, and 98% of the normalized resistance were examined as different critical-temperature definitions.

Bulk magnetic susceptibility measurements reproduced the same *relative* change in the superconducting transition temperature under $(001)_t$ tensile stress as compared to those changes determined from the resistance traces [Fig. 2(a) and Fig. S7]. This similarity ruled out filamentary behavior that otherwise would have resulted in tremendously reduced screening [48–50]. Instead, we concluded that the gap between the magnetic and transport transitions was a signature of the "extreme type-II" nature of superconductivity in STO [31,46,51], meaning that the combination of the extremely low superfluid density and mobile vortices makes STO exceptionally susceptible to external perturbations. Additionally, local susceptometry in previous works indicated that the crossover from the bulk superconducting behavior to island-like (percolative) behavior occurs fairly abruptly within ~10 mK in unstrained bulk STO [52] of similar quality to the crystals studied here. The same conclusions about the large change in the critical temperature of STO crystals as a result of the applied stress in our work were reached irrespective of the $T_c$ definition used [Fig. 2(b)]. The effect was evident only in crystals with preferentially oriented domains (optical microscope images appear in the supplemental material, Fig. S6).

Lower-doping and higher-doping samples underwent some increase in $T_c$ under strain [Figs. 3(a) and 3(d)], but they had higher crystal brittleness [maximum strains are shown in Figs. 3(a) and 3(d)], limiting the strain that we could

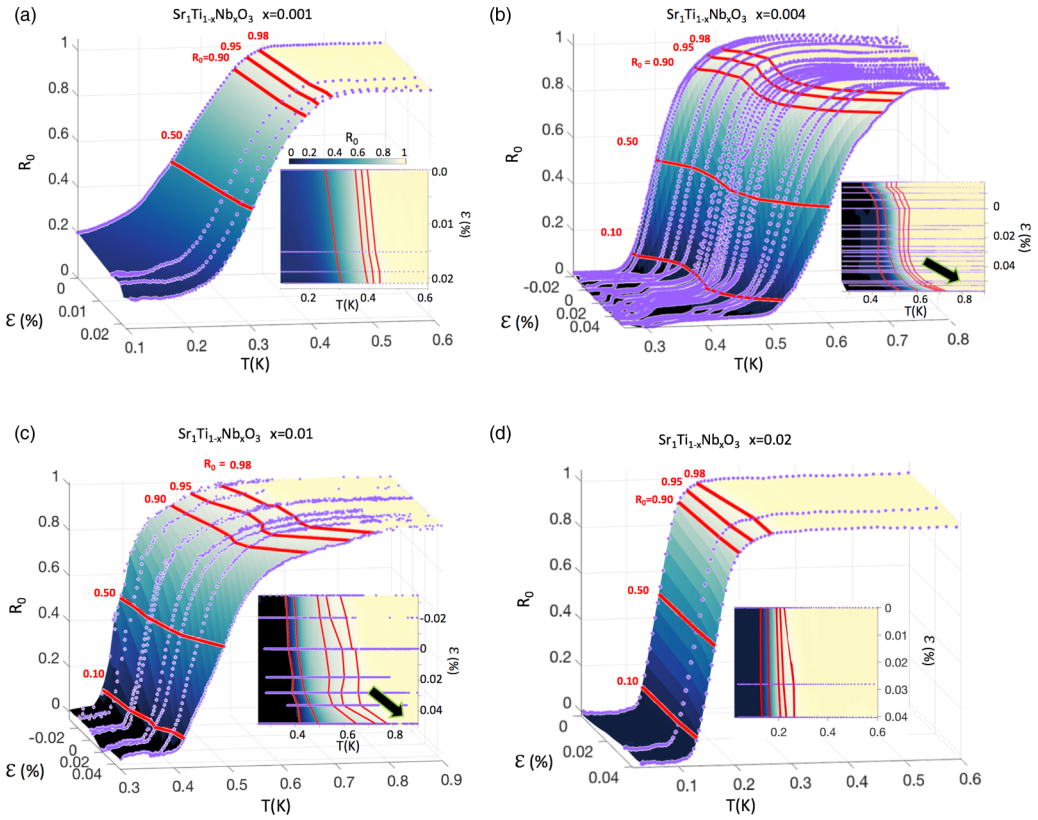


FIG. 3. Doping dependence of the increase in the onset of the superconducting transition under tension. (a)–(d) Representative resistance data for $Sr_1Ti_{1-x}Nb_xO_3$ crystals with four doping levels ($x = 0.001$, 0.004, 0.01, and 0.02) spanning a large portion of the phase space. The main panels show resistive transitions (purple dots on linearly interpolated colormaps) normalized to resistances at 1 K. The red lines in the main panels and insets depict equal-resistance contours that define $T_c$ at 10%, 50%, 90%, 95%, and 98% of the normalized resistance $R_0$. Lower-doping samples [(a), $x = 0.001$] showed a mild enhancement only; they often fractured (usually normal to the strain axis) at intermediate strains of ~0.02%. Near-optimally-doped samples [(b) and (c); $x = 0.04$ and 0.01, respectively] displayed a large and divergent-like increase in $T_c$ (arrows). Note that the sample in Fig. 2 did not reach high enough strains to manifest divergent-like behavior (within the strain error bars of approximately 0.01%). The overdoped sample [(d), $x = 0.02$] exhibited almost no increase in $T_c$ (similar to other samples with the same doping, data not shown). The normal resistance values defined at 1 K appear in the supplemental material (Fig. S9). Some sample-to-sample variations apparently arise from imperfections in the sample mounting and wire-bonding rather than the compositions of the samples. All of the above definitions of $T_c$ yielded a consistent picture of enhanced $T_c$ with slight sample-to-sample variations, as expected from our experimental design and setup.

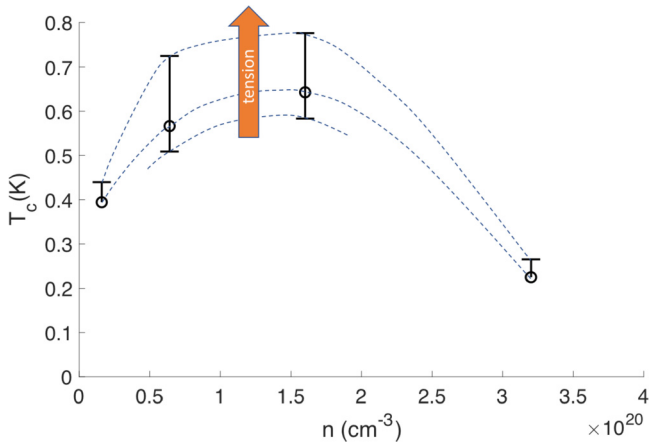


FIG. 4. Large increase in the onset of the superconducting transition and general enhancement of $T_c$ across the phase diagram. $T_c$ is shown as a function of doping; this figure summarizes the (001) stress data from the four samples depicted in Fig. 3 ($x = 0.001$, 0.004, 0.01, and 0.02). The plotted "error bars" are ranges of $T_c$ defined as $0.98R_n$ at smallest-to-largest strains (Table I). Dashed lines are guides to the eye. The width of the transition increased insubstantially or remained largely unaffected by strain. These data reveal anomalous $T_c$ growth that is among the highest that was detected in many conventional and unconventional superconductors [43,55–60] in relative terms under given strain.

induce [53]. In general, we achieved higher strains in samples with higher Nb content (and higher carrier concentrations; Table S1 of the supplemental material contains basic sample parameters). "Overdoped" samples [e.g., Fig. 3(d)] did not exhibit a substantial increase in $T_c$. Thus, the highest starting $T_c$ and strongest increase in $T_c$ occurred in nearly optimally doped samples [Figs. 3(b) and 3(c)]. The enhanced $T_c$ is summarized as a "dome" phase diagram in Fig. 4, as well as in Table I with all definitions of $T_c$ yielding a similar enhancement under tensile strain.

There was an apparent sample-to-sample (or experiment-to-experiment) variation in the details of the transition, in particular how smoothly the last stage of the transition to the zero-resistance state occurred. The samples in Fig. 2 displayed sharper and "cleaner" transitions than other samples with the same Nb content shown in Figs. 3(b) and 3(c). The difference between the datasets is the position of the measurement wire-bond leads: they were bonded closer to the middle of the samples whose data are plotted in Fig. 2 but closer to the mounting ends, near the strain cell clamps, for Fig. 3. We attribute an inhomogeneous strain or pinned tetragonal domains near the mounting ends as being responsible for the less homogeneous transition signatures of these samples.

We also note that the diamagnetic screening signal in Fig. 2 extends all the way into the resistive drop (for the out-of-phase susceptibility, see Fig. S7); this observation was confirmed in additional samples and other doping levels (Fig. S8). This observation differs from those of some previous studies, which reported a larger apparent gap between magnetic and resistive data, e.g., Ref. [23]. To have less of an influence on the responses of the sample in the transition region, we typically applied only 10 $\mu$A transport current and only a 5 mG magnetic field amplitude at 200 kHz.

We also found that the critical temperature of $SrTi_{1-x}Nb_xO_3$ decreases under small compressive (001) strain for nearly or higher-than-optimal doping levels [Figs. 3(b), 3(c), 4, and Table I], consistent with previous studies of multidomain samples [33]. Under small compressions in the (001) direction, the samples may host all possible domains, with the AFD $c$-axis pointing in the [100], [010], and [001] directions; this geometry may be inconclusive. However, at larger compressive (001) strains we observed a mild relative enhancement in $T_c$, as reported elsewhere [54].

## IV. DISCUSSION

We now discuss the hypothesis that FE instability drives superconductivity in STO. Previous works reported that deformation geometries in which the $c$-axis elongates and the oxygen octahedra are rotated further from their equilibrium AFD angle enhance FE instability [36,41,61]. Similarly, in our geometry, the $(001)_t$ tensile stress in crystals not only promotes elongation of the $c$-axis due to the Sr matrix deformation, but also causes the oxygen octahedra to rotate further [61]. The additional rotation of the octahedra is on the order of 0.5° to 1° (estimated assuming $c$-axis strains of ∼0.07% [61]). This AFD rotation and $c$-axis elongation may lead to a softening of the FE mode on the order of 1 THz, which is enough to considerably soften the FE mode [62,63] and thus substantially enhance $T_c$, according to the FE mode scenario.

The increase of $T_c$ upon tuning toward ferroelectricity has been captured in a recent model of FE phonon-mediated coupling [3,7]. In this model, $T_c$ is expected to grow sharply as the phonon mode frequency decreases on the approach to the incipient FE quantum phase transition. It is very likely that the sharp upturn in $T_c$ in our data is the start of the singularity (Fig. S1) that would occur if the quantum phase transition occurred near these strains. Another observation consistent with the model is that the overdoped samples [Fig. 3(d)] responded very weakly to strain even for relatively large strains, probably

TABLE I. Summary of $T_c$ at extreme and zero strains for the four samples depicted in Fig. 3 ($x = 0.001$, 0.004, 0.01, and 0.02), defined at different $R_n$ levels.

| $n(10^{20}\,\mathrm{cm}^{-3})$ | 0.16 | | 0.64 | | | 1.6 | | | 3.2 | |
|---|---|---|---|---|---|---|---|---|---|---|
| $\varepsilon$ (%) | 0 | 0.0221 | −0.034 | 0 | −0.048 | −0.029 | 0 | 0.066 | 0 | 0.04 |
| $T_c$ (mK) at $0.1R_n$ | – | – | 365 | 420 | 530 | 363 | 380 | 420 | 128 | 134 |
| $T_c$ (mK) at $0.5R_n$ | 252 | 310 | 403 | 462 | 600 | 396 | 414 | 500 | 158 | 166 |
| $T_c$ (mK) at $0.98R_n$ | 395 | 440 | 509 | 566 | 725 | 583 | 643 | 776 | 225 | 265 |

because the overdoped samples are farther away in the phase space from the expected polar phase transition than less-doped samples (see the model in Ref. [7] and the Supplemental Material).

Comparing our $(001)_t$ tensile stress data with a calculated trend in the FE phonon modes [Fig. 1(b) and Fig. S1] demonstrates that the increase in $T_c$ is correlated with the expected softening of the transverse FE phonon mode whose polarization is parallel both to the AFD axis and the applied stress [Fig. 1(a)], the so-called $A_{2u}$ mode [35] (details in the supplemental material). The asymmetric behavior of $T_c$ under stress or strain inversion in STO is nontrivial. The FE phonon modes perpendicular to the AFD (and stress) axis are expected to harden under tension and soften under compression (Fig. 1), while the modes with the perpendicular polarization behave in the opposite manner [64]. Our data indicate that $T_c$ could be linked specifically to the mode with polarization parallel to the AFD axis [Figs. 1(a) and 1(b)].

The strength of the response and the maximum $T_c$ and strain appear to correlate with the dome of the critical temperature (Fig. 4). The strongest response was near optimal doping, and the weakest near maximum doping (Fig. 4). One possible interpretation is that the response is strongest near—but slightly off—the FE critical point (as would be defined for undoped samples). At locations too close to the critical point, there are not enough carriers to produce robust superconducting stiffness; very far from the critical point, the dopants dampen and screen the FE fluctuations too much and thus suppress superconductivity. Therefore, the maximum $T_c$ and strength of the response are expected to occur slightly closer to the undoped side.

The above interpretation is in qualitative agreement with our data. However, on a quantitative level, the seemingly weaker transverse FE phonon-electron mode coupling, as compared to the longitudinal mode coupling, has been debated [8,65]. This subject of further investigation requires the development of a full microscopic model that includes the anharmonic modes that are expected at the FE transition. Developing such a microscopic model is well beyond the scope of the current *experimental* work. However, to guide future efforts, we point out that the longitudinal mode is generally not coupled to strain [35], and therefore a full explanation of our results by models based on the longitudinal mode only is not sufficient; a role of the transverse modes is not excluded. For example, a recently proposed two-phonon electron-phonon coupling mechanism could be the key to a more quantitative model [12]. Additionally, the effect of increasing $T_c$ is evident at fairly high doping, where the multibands and the anisotropy [28,66–68] should not play a major role under these tiny strains (see the supplemental material).

The smallness of the maximal strains (0.05–0.07 %) and the corresponding tiny unit-cell deformations (on the order of ∼0.2 pm)—which cause changes in $T_c$ of tens of percent—may seem surprising. This behavior is quite sensitive, given that in many other works on different materials the strains needed to be about an order of magnitude larger in order for $T_c$ to appreciably change [55–59,69]. On the other hand, significantly enhanced response to strain is known to occur near other phase transitions, e.g., in a topological transition [43]. More relevant to our work, such small strains have been shown to lead to a tenfold or more softening of the FE mode under strain [35–39,41]. To our knowledge, this parameter is the only one to change so dramatically in STO under such small strains. We conclude that the FE polarization can have a dramatic effect on the electron pairing properties, even with very small picometer-scale lattice distortions [40].

In future works, it will be important to address the temperature dependence of the normal state resistance [70] in a large temperature range under uniaxial stress. Direct phonon measurement and manipulation techniques, combined with probes such as electronic transport and scanning SQUID imaging [71], could bring to life new ideas such as probing very high *dynamic* strain responses, potentially leading to even higher values of $T_c$ than those accessible with the static strains used in this work.

## V. CONCLUSION

The results presented here open an avenue for investigations of the interplay between superconductivity and strain and pressure effects. Our interpretation of the higher $T_c$ observed here underscores the importance of the FE soft mode for superconductivity in STO and suggests that the structural AFD order cooperates with the FE order. Our data show consistent behavior across the entire range of carrier concentrations for which superconductivity occurs, with quantitative variations. Current theoretical descriptions of the mechanism of superconductivity in STO [3–7,9,10,12,34] do not account for the important interplay between incipient [72] ferroelectricity [18] and structural conditions highlighted here. These findings should provide key inputs for future theoretical models that aim to explain the interplay between superconductivity and other orders in STO. Our work and the surge of experimental studies of other superconducting compounds under stresses [73–75,60] vividly demonstrate that strain is a promising control parameter to make significant advances in tuning quantum materials.

## ACKNOWLEDGMENTS

We thank J. Hancock, J. Levy, Y. Kedem, N. Spaldin, J. Budnick, and B. Wells for helpful discussions, J. Sheldon and B. Hines for help with setting up the experiments, and B. Willis for use of equipment to make leads to the samples. The State of Connecticut, the Physics Department, and the Vice Provost for Research at the University of Connecticut provided financial support through research startup funds. The Scholarship Facilitation award also provided funding to C.H. The College for Liberal Arts and Sciences at the University of Connecticut awarded C.H. a graduate student financial award. The work of J.C. was supported by the Mark Miller award. A.V.B. and K.D. were supported by U.S. BES E3B7, VILLUM FONDEN via the Centre of Excellence for Dirac Materials (Grant No. 11744), and by the Knut and Alice Wallenberg Foundation (2013.0096).

[1] J. Appel, Phys. Rev. **180**, 508 (1969).
[2] Y. Takada, J. Phys. Soc. Jpn. **49**, 1267 (1980).
[3] J. M. Edge, Y. Kedem, U. Aschauer, N. A. Spaldin, and A. V. Balatsky, Phys. Rev. Lett. **115**, 247002 (2015).
[4] J. Ruhman and P. A. Lee, Phys. Rev. B **94**, 224515 (2016).
[5] L. P. Gor'kov, Proc. Natl. Acad. Sci. (USA) **113**, 4646 (2016).
[6] L. P. Gor'kov, J. Supercond. Nov. Mag. **30**, 845 (2017).
[7] K. Dunnett, A. Narayan, N. A. Spaldin, and A. V. Balatsky, Phys. Rev. B **97**, 144506 (2018).
[8] P. Wölfle and A. V. Balatsky, Phys. Rev. B **98**, 104505 (2018).
[9] Y. Kedem, Phys. Rev. B **98**, 220505 (2018).
[10] J. R. Arce-Gamboa and G. G. Guzmán-Verri, Phys. Rev. Mater. **2**, 104804 (2018).
[11] M. N. Gastiasoro, A. V. Chubukov, and R. M. Fernandes, Phys. Rev. B **99**, 094524 (2019).
[12] D. van der Marel, F. Barantani, and C. W. Rischau, Phys. Rev. Res. **1**, 013003 (2019).
[13] A. Stucky, G. W. Scheerer, Z. Ren, D. Jaccard, J.-M. Poumirol, C. Barreteau, E. Giannini, and D. van der Marel, Sci. Rep. **6**, 37582 (2016).
[14] C. W. Rischau, X. Lin, C. P. Grams, D. Finck, S. Harms, J. Engelmayer, T. Lorenz, Y. Gallais, B. Fauqué, J. Hemberger, and K. Behnia, Nat. Phys. **13**, 643 (2017).
[15] Y. Tomioka, N. Shirakawa, K. Shibuya, and I. H. Inoue, Nat. Commun. **10**, 738 (2019).
[16] K. Ahadi, L. Galletti, Y. Li, S. Salmani-Rezaie, W. Wu, and S. Stemmer, Sci. Adv. **5**, eaaw0120 (2019).
[17] W. G. Stirling, J. Phys. C **5**, 2711 (1972).
[18] K. A. Müller and H. Burkard, Phys. Rev. B **19**, 3593 (1979).
[19] Y. Fujii, H. Uwe, and T. Sakudo, J. Phys. Soc. Jpn. **56**, 1940 (1987).
[20] D. Lee, H. Lu, Y. Gu, S.-Y. Choi, S.-D. Li, S. Ryu, T. R. Paudel, K. Song, E. Mikheev, S. Lee, S. Stemmer, D. A. Tenne, S. H. Oh, E. Y. Tsymbal, X. Wu, L.-Q. Chen, A. Gruverman, and C. B. Eom, Science **349**, 1314 (2015).
[21] R. T. Brierley and P. B. Littlewood, Phys. Rev. B **89**, 184104 (2014).
[22] J. F. Schooley, W. R. Hosler, E. Ambler, J. H. Becker, M. L. Cohen, and C. S. Koonce, Phys. Rev. Lett. **14**, 305 (1965).
[23] C. S. Koonce, M. L. Cohen, J. F. Schooley, W. R. Hosler, and E. R. Pfeiffer, Phys. Rev. **163**, 380 (1967).
[24] N. Reyren, S. Thiel, A. D. Caviglia, L. F. Kourkoutis, G. Hammerl, C. Richter, C. W. Schneider, T. Kopp, A.-S. Rüetschi, D. Jaccard, M. Gabay, D. A. Muller, J.-M. Triscone, and J. Mannhart, Science **317**, 1196 (2007).
[25] C. Richter, H. Boschker, W. Dietsche, E. Fillis-Tsirakis, R. Jany, F. Loder, L. F. Kourkoutis, D. A. Muller, J. R. Kirtley, C. W. Schneider, and J. Mannhart, Nature (London) **502**, 528 (2013).
[26] E. Maniv, M. B. Shalom, A. Ron, M. Mograbi, A. Palevski, M. Goldstein, and Y. Dagan, Nat. Commun. **6**, 8239 (2015).
[27] X. Lin, G. Bridoux, A. Gourgout, G. Seyfarth, S. Krämer, M. Nardone, B. Fauqué, and K. Behnia, Phys. Rev. Lett. **112**, 207002 (2014).
[28] X. Lin, A. Gourgout, G. Bridoux, F. Jomard, A. Pourret, B. Fauqué, D. Aoki, and K. Behnia, Phys. Rev. B **90**, 140508 (2014).
[29] S. E. Rowley, C. Enderlein, J. F. de Oliveira, D. A. Tompsett, E. B. Saitovitch, S. S. Saxena, and G. G. Lonzarich, arXiv:1801.08121(Cond-Mat).
[30] C. Collignon, X. Lin, C. W. Rischau, B. Fauqué, and K. Behnia, Annu. Rev. Condens. Matter Phys. **10**, 25 (2018).
[31] J. F. Schooley, W. R. Hosler, and M. L. Cohen, Phys. Rev. Lett. **12**, 474 (1964).
[32] E. R. Pfeiffer and J. F. Schooley, Phys. Rev. Lett. **19**, 783 (1967).
[33] E. R. Pfeiffer and J. F. Schooley, J. Low Temp. Phys. **2**, 333 (1970).
[34] S. N. Klimin, J. Tempere, J. T. Devreese, J. He, C. Franchini, and G. Kresse, J. Supercond. Novel Magn. **32**, 2739 (2019).
[35] H. Uwe and T. Sakudo, Phys. Rev. B **13**, 271 (1976).
[36] J. H. Haeni, P. Irvin, W. Chang, R. Uecker, P. Reiche, Y. L. Li, S. Choudhury, W. Tian, M. E. Hawley, B. Craigo, A. K. Tagantsev, X. Q. Pan, S. K. Streiffer, L. Q. Chen, S. W. Kirchoefer, J. Levy, and D. G. Schlom, Nature (London) **430**, 758 (2004).
[37] F. He, B. O. Wells, Z.-G. Ban, S. P. Alpay, S. Grenier, S. M. Shapiro, W. Si, A. Clark, and X. X. Xi, Phys. Rev. B **70**, 235405 (2004).
[38] F. He, B. O. Wells, and S. M. Shapiro, Phys. Rev. Lett. **94**, 176101 (2005).
[39] Y. L. Li, S. Choudhury, J. H. Haeni, M. D. Biegalski, A. Vasudevarao, A. Sharan, H. Z. Ma, J. Levy, V. Gopalan, S. Trolier-McKinstry, D. G. Schlom, Q. X. Jia, and L. Q. Chen, Phys. Rev. B **73**, 184112 (2006).
[40] S. Ismail-Beigi, F. J. Walker, A. S. Disa, K. M. Rabe, and C. H. Ahn, Nat. Rev. Mater. **2**, 17060 (2017).
[41] B. S. de Lima, M. S. da Luz, F. S. Oliveira, L. M. S. Alves, C. A. M. dos Santos, F. Jomard, Y. Sidis, P. Bourges, S. Harms, C. P. Grams, J. Hemberger, X. Lin, B. Fauqué, and K. Behnia, Phys. Rev. B **91**, 045108 (2015).
[42] C. W. Hicks, D. O. Brodsky, E. A. Yelland, A. S. Gibbs, J. A. N. Bruin, M. E. Barber, S. D. Edkins, K. Nishimura, S. Yonezawa, Y. Maeno, and A. P. Mackenzie, Science **344**, 283 (2014).
[43] A. Steppke, L. Zhao, M. E. Barber, T. Scaffidi, F. Jerzembeck, H. Rosner, A. S. Gibbs, Y. Maeno, S. H. Simon, A. P. Mackenzie, and C. W. Hicks, Science **355**, 148 (2017).
[44] C. A. Watson, A. S. Gibbs, A. P. Mackenzie, C. W. Hicks, and K. A. Moler, Phys. Rev. B **98**, 094521 (2018).
[45] D. Davino, J. Franklin, and I. Sochnikov, arXiv:1912.08299, AIP Adv., doi: 10.1063/1.5130383.
[46] C. Herrera and I. Sochnikov, J. Supercond. Nov. Magn. (2019), doi:10.1007/s10948-019-05282-7.
[47] B. Lautrup, *Physics of Continuous Matter: Exotic and Everyday Phenomena in the Macroscopic World*, 2nd ed. (CRC Press, Boca Raton, FL, 2011).
[48] S. Nagata, S. Ebisu, T. Aochi, Y. Kinoshita, S. Chikazawa, and K. Yamaya, J. Phys. Chem. Solids **52**, 761 (1991).
[49] D. Pelc, Z. Anderson, B. Yu, C. Leighton, and M. Greven, arXiv:1808.05763 (Cond-Mat).
[50] T. M. Bretz-Sullivan, A. Edelman, J. S. Jiang, A. Suslov, D. Graf, J. Zhang, G. Wang, C. Chang, J. E. Pearson, A. B. Martinson, P. B. Littlewood, and A. Bhattacharya, arXiv:1904.03121 (Cond-Mat).
[51] A. Leitner, D. Olaya, C. T. Rogers, and J. C. Price, Phys. Rev. B **62**, 1408 (2000).
[52] H. Noad, E. M. Spanton, K. C. Nowack, H. Inoue, M. Kim, T. A. Merz, C. Bell, Y. Hikita, R. Xu, W. Liu, A. Vailionis, H. Y. Hwang, and K. A. Moler, Phys. Rev. B **94**, 174516 (2016).
[53] A. Nakamura, K. Yasufuku, Y. Furushima, K. Toyoura,. K. Lagerlöf, and K. Matsunaga, Crystals **7**, 351 (2017).

[54] C. Herrera and I. Sochnikov, J. Supercond. Nov. Magn. (2019), doi:10.1007/s10948-019-05256-9.
[55] M. Mito, K. Ogata, H. Goto, K. Tsuruta, K. Nakamura, H. Deguchi, T. Horide, K. Matsumoto, T. Tajiri, H. Hara, T. Ozaki, H. Takeya, and Y. Takano, Phys. Rev. B **95**, 064503 (2017).
[56] O. M. Dix, A. G. Swartz, R. J. Zieve, J. Cooley, T. R. Sayles, and M. B. Maple, Phys. Rev. Lett. **102**, 197001 (2009).
[57] C. L. Watlington, J. W. Cook, and M. J. Skove, Phys. Rev. B **15**, 1370 (1977).
[58] V. I. Dotsenko, I. F. Kislyak, V. T. Petrenko, M. A. Tikhonovsky, A. M. Shkilko, L. N. Zagoruiko, and L. M. Rogozyanskaya, Cryogenics **41**, 225 (2001).
[59] K. Kikuchi, T. Isono, M. Kojima, H. Yoshimoto, T. Kodama, W. Fujita, K. Yokogawa, H. Yoshino, K. Murata, T. Kaihatsu, H. Akutsu, and J. Yamada, J. Am. Chem. Soc. **133**, 19590 (2011).
[60] M. D. Bachmann, G. M. Ferguson, F. Theuss, T. Meng, C. Putzke, T. Helm, K. R. Shirer, Y.-S. Li, K. A. Modic, M. Nicklas, M. König, D. Low, S. Ghosh, A. P. Mackenzie, F. Arnold, E. Hassinger, R. D. McDonald, L. E. Winter, E. D. Bauer, F. Ronning, B. J. Ramshaw, K. C. Nowack, and P. J. W. Moll, Science **366**, 221 (2019).
[61] U. Aschauer and N. A. Spaldin, J. Phys.: Condens. Matter **26**, 122203 (2014).
[62] M. Takesada, M. Itoh, and T. Yagi, Phys. Rev. Lett. **96**, 227602 (2006).
[63] Y. Tsujimi, T. Yanagisawa, and T. Mogami, J. Kor. Phys. Soc. **62**, 1014 (2013).
[64] D. Nuzhnyy, J. Petzelt, S. Kamba, T. Yamada, M. Tyunina, A. K. Tagantsev, J. Levoska, and N. Setter, J. Electroceram. **22**, 297 (2009).
[65] J. Ruhman and P. A. Lee, arXiv:1901.11065 (Cond-Mat).
[66] C. Collignon, B. Fauqué, A. Cavanna, U. Gennser, D. Mailly, and K. Behnia, Phys. Rev. B **96**, 224506 (2017).
[67] M. Thiemann, M. H. Beutel, M. Dressel, N. R. Lee-Hone, D. M. Broun, E. Fillis-Tsirakis, H. Boschker, J. Mannhart, and M. Scheffler, Phys. Rev. Lett. **120**, 237002 (2018).
[68] A. G. Swartz, H. Inoue, T. A. Merz, Y. Hikita, S. Raghu, T. P. Devereaux, S. Johnston, and H. Y. Hwang, Proc. Natl. Acad. Sci. (USA) **115**, 1475 (2018).
[69] M. Mito, H. Matsui, K. Tsuruta, T. Yamaguchi, K. Nakamura, H. Deguchi, N. Shirakawa, H. Adachi, T. Yamasaki, H. Iwaoka, Y. Ikoma, and Z. Horita, Sci. Rep. **6**, 36337 (2016).
[70] X. Lin, B. Fauqué, and K. Behnia, Science **349**, 945 (2015).
[71] I. Sochnikov, L. Maier, C. A. Watson, J. R. Kirtley, C. Gould, G. Tkachov, E. M. Hankiewicz, C. Brüne, H. Buhmann, L. W. Molenkamp, and K. A. Moler, Phys. Rev. Lett. **114**, 066801 (2015).
[72] S. U. Handunkanda, E. B. Curry, V. Voronov, A. H. Said, G. G. Guzmán-Verri, R. T. Brierley, P. B. Littlewood, and J. N. Hancock, Phys. Rev. B **92**, 134101 (2015).
[73] J.-H. Chu, H.-H. Kuo, J. G. Analytis, and I. R. Fisher, Science **337**, 710 (2012).
[74] A. P. Drozdov, M. I. Eremets, I. A. Troyan, V. Ksenofontov, and S. I. Shylin, Nature (London) **525**, 73 (2015).
[75] J. T. Sypek, H. Yu, K. J. Dusoe, G. Drachuck, H. Patel, A. M. Giroux, A. I. Goldman, A. Kreyssig, P. C. Canfield, S. L. Bud'ko, C. R. Weinberger, and S.-W. Lee, Nat. Commun. **8**, 1083 (2017).
[76] See Supplemental Material at http://link.aps.org/supplemental/10.1103/PhysRevMaterials.3.124801 for further experimental details, and additional discussions.